Flomeko 2000 - IMEKO TC9 Conference
Salvador, Bahia, BRAZIL
4-8 June, 2000

3D VELOCITY PROFILE RECONSTRUCTION OF GAS FLOW IN A PIPE WITH ULTRASONIC TOMOGRAPHY

J. Escande, P. Gajan, A. Strzelecki
French Agency for Aerospace Research (ONERA)
BP 4025, 31055 Toulouse Cedex 4, France

Abstract: *Beyond possibilities of simple flowmeters, ultrasonic tomography allows to reconstitute the three-dimensional velocity field over a circular pipe cross section. The differences of transit times between transducers distributed around the pipe are used in an iterative algebraic reconstruction algorithm in order to reconstruct the three velocity components. This experimental method has been tested successfully to quantify the 3D velocity field of various flows (fully developed, asymmetric and swirling air flows).*

Keywords: Tomography, Ultrasonic, Diagnostic, Gas Flow, Velocity Profiles, Pipe

1 INTRODUCTION

Multipath ultrasonic transit time meters for gas flow measurement (USM) have been developed to such a stage that they can be considered as alternatives to the more conventional orifice plate and turbine meters for fiscal metering. As a comparison to other conventional meters, the USM technology offers significant advantages such as compactness, bi-directionality, short upstream and downstream requirements with respect to bends, no pressure loss and fast response. The first generations of ultrasonic meters have been on the market for about 5-10 years, and have demonstrated their capability to provide satisfying metering accuracy. In appropriate applications, multipath ultrasonic meters offer cost benefits [1].

Furthermore, a lot of papers have shown that it is possible to obtain a better accuracy and a superior diagnostic ability with a multipath meter compared to those related to a single path [2] [3] [4].

Using the principle of the USM with numerous differences in transit times given by multiple transducers pairs, one can reconstruct the three components of the velocity field through a test section of the pipe. This technique, called "Ultrasonic Tomography", has only been developed in laboratory environment. This present work has been carried out in order to apply tomography to the diagnostic of *in situ* industrial gas flows.

First of all, we had reached this goal for transversal components and a paper was presented at FLOMEKO'98 [5]. The experimental results allowed us to validate the developed tomographic system in the case of swirling air flows. Since, we have extended the technique in order to reconstruct the axial velocity profile of fully developed flows, swirling flows and asymmetric flows. In order to verify the reliability of the developed device, these flows have been measured and compared to a hot wire characterisation.

The basic principles of the ultrasonic flowmeter and tomography are described. Then, we explain how to resolve the resulting equations with a reconstruction algorithm using the transit times measurements. Finally, we present experimental validations of this technique.

2 ULTRASONIC FLOWMETER PRINCIPLE

Ultrasonic flowmeters measure the mean velocity of a flow from the modification of the sound velocity in it. If the wave propagates in the flow direction, the sound velocity increases ;otherwise, it decreases. Of course, this phenomena appears if the direction of propagation of the wave is not perpendicular to the flow direction. For this reason, in ultrasonic flowmeters, the couple of ultrasonic transducers is inclined at an angle q with respect to the pipe axes as it is shown in figure 1.

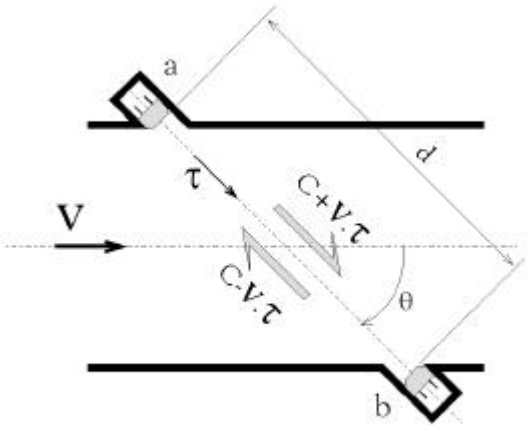

Figure 1. Ultrasonic flowmeter principle.

The time of flight of the wave from the upstream transducer *a* to the downstream one *b*, is given by the following equation :

$$t_{ab} = \int_a^b \frac{ds}{C + \mathbf{V} \cdot t} \tag{1}$$

and in the other direction :

$$t_{ba} = \int_a^b \frac{ds}{C - \mathbf{V} \cdot t} \tag{2}$$

In many cases, the flow velocity can be considered to be much smaller than the sound speed, as a result these two expressions become :

$$t_{ab} = \frac{1}{C}\int_a^b \left(1 - \frac{\mathbf{V} \cdot t}{C}\right) ds \quad \text{and} \quad t_{ba} = \frac{1}{C}\int_a^b \left(1 + \frac{\mathbf{V} \cdot t}{C}\right) ds \tag{3) and (4}$$

Now, subtracting (4) from (3) and introducing *d* as the distance between the two transducers, it is possible to get the bulk (or mean) velocity V_m of the flow :

$$Dt = t_{ab} - t_{ba} = \frac{-2}{C^2}\int_a^b \mathbf{V} \cdot t ds = \frac{-2dV_m \cos q}{C^2} \tag{5}$$

3 ULTRASONIC TOMOGRAPHY PRINCIPLE

The principle of the tomography consists in processing many transit times Dt obtained on numerous ultrasonic lines to determine the velocity profile through a pipe section. Ultrasonic lines are materialised by a couple of source/receiver transducers. To get the three velocity components, Johnson *et al.* [6] suggested the transducers distribution of the figure 2.

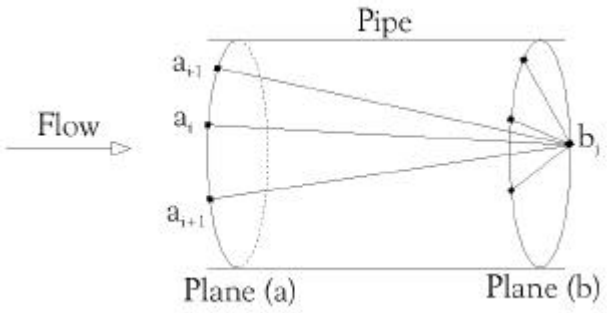

Figure 2. Transducers distribution on a pipe.

Assuming that the flow conditions do not change between planes (*a*) and (*b*), the set of pairs (a_i,a_j) allows the reconstruction of transversal components of the flow, while the pairs (a_i,b_j) are used for the axial component.

The time of flight difference between the transducer a_i and the transducer b_j, is expressed by an expression similar to equation (5). One has only to put a_i in place of *a*, b_j in place of *b*. The unit vector $\boldsymbol{t}$ tangent to ultrasonic ray has to be expressed in the cartesian coordinate system ($\boldsymbol{x}$,$\boldsymbol{y}$,$\boldsymbol{z}$), with the z-axis orientated along the pipe axis, by the following expression :

$$\boldsymbol{t} = (\mathbf{x}\cos\theta + \mathbf{y}\sin\theta)\sin\gamma + \mathbf{z}\cos\gamma \tag{6}$$

where γ is the angle between $\boldsymbol{z}$ and $\boldsymbol{t}$ and, θ is the angle between $\boldsymbol{x}$ and $\boldsymbol{r}$, $\boldsymbol{r}$ being the projection of $\boldsymbol{t}$ on the plane (*xOy*),

So, we obtain the new expression :

$$\Delta t = T_0(a_i, b_j) = \frac{-2}{C^2}\int_{a_i}^{b_j}\left[\left(V_x\cos\theta + V_y\sin\theta\right)\sin\gamma + V_z\cos\gamma\right]ds \tag{7}$$

In the same way, an expression can be derived for a time of flight difference measured in the plane (*a*) only :

$$T_1(a_i, a_j) = \frac{-2}{C^2}\int_{a_i}^{a_j}\left(V_x\cos\theta + V_y\sin\theta\right)dr \tag{8}$$

If a_j is the projection of b_j along the cylindrical axis onto the plane (*a*), Johnson *et al.* [6] define the fictitious time as :

$$T_2(a_i, b_j) = T_0(a_i, b_j) - T_1(a_i, a_j) = \frac{-2\cot\alpha\gamma}{C^2}\int_{a_i}^{b_j} V_z ds \tag{9}$$

which allows one to reconstruct the component V_z independently from the transversal components of the flow.

4 ALGORITHM OF RECONSTRUCTION

When we get all necessary transit time differences, these data have to be processed in order to reconstruct the initial speed profile.

The reconstruction algorithm used here is a combination of the approach of Johnson *et al.* [6] and Herman's [8]. In fact, the integral in equation (8) is written in terms of an approximate sum by subdividing the segment $[a_i a_j]$ into elements of approximately constant length ΔL. The velocity is considered constant along each element and equal to its value at the middle point *V(x,y)*. But, the reconstruction can only be done for a finite number of points which are the nodes of a square grid of discretisation of the test section. Therefore, the velocity *V* of any point *(x,y)* placed in a mesh defined

by the four speeds [V_1, V_2, V_3, V_4] is expressed by the bilinear interpolation described in figure 3, expressed as followed :

$$\begin{cases} V(x,y) = e_{i,j}V_{i,j} + e_{i,j+1}V_{i,j+1} + e_{i+1,j}V_{i+1,j} + e_{i+1,j+1}V_{i+1,j+1} \\ e_{i,j} + e_{i,j+1} + e_{i+1,j} + e_{i+1,j+1} = 1 \end{cases} \quad (10)$$

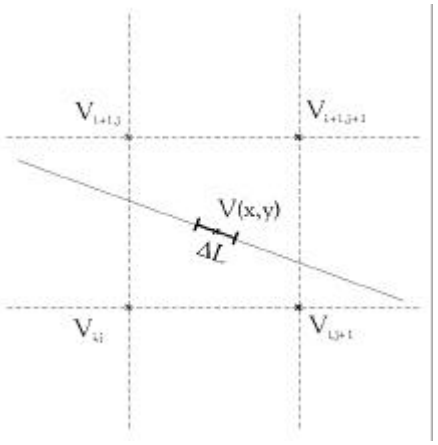

Figure 3. Bilinear interpolation on a cartesian mesh.

So, considering all the ultrasonic beams, equation (8) can become a set of linear equations [9] as :

$$A_{xy}V_{xy} = T_{xy} \quad (11)$$

where A_{xy} is a matrix built from the mathematical decomposition of integral lines (8) from every transducers couples, T_{xy} a column vector containing all transit time differences measured, and V_{xy} the column vector corresponding to the solution, that is to say, the velocity on each point of the mesh.

If there are N_{xy} nodes into the pipe, V_{xy} gets $2\ N_{xy}$ coefficients with the N_{xy} first ones for the V_x component and the next N_{xy} ones for V_y component.

A second set of linear equations is obtained for the axial flow from the discretisation of equation (9):

$$A_zV_z = T_z \quad (12)$$

If there are N_z nodes into the pipe, V_z gets N_z coefficients for the V_z component. So logically $N_z > N_{xy}$. For instance, a reconstruction made with 126 equations (i.e. 126 transit times measured) give a 10×10 mesh for the secondary flow (N_{xy} = 10) and a 14×14 mesh for the secondary flow (N_z = 14).

Considering the flow turbulence, in order to solve the systems (11) and (12), one has to use an iterative algorithm to minimise the inaccuracy on time of flight measurement. This is the reason why a quasi-solution algorithm, called " conjugate gradient method ", is used here.

To validate the algorithm, computer simulations have been realised on theoretical velocity profiles [5].

5 TIME OF FLIGHT EVALUATION

In order to make an effective tomography, it is necessary to increase the number of ultrasonic paths (see figure 2) in order to cover the maximum of the test section. Moreover, because of the acoustic impedance difference between the gas and the pipe metal which highly attenuates the acoustic wave, transducers are installed directly in contact with the fluid. Figure 4 represents the plane (*a*) of figure 2 with 12 transducers around the section. Lines materialise theoretic ultrasonic rays defined by one receiver and seven sources. Each of these couples defines one transit time difference $T_1(a_i,a_j)$ given by relation (8).

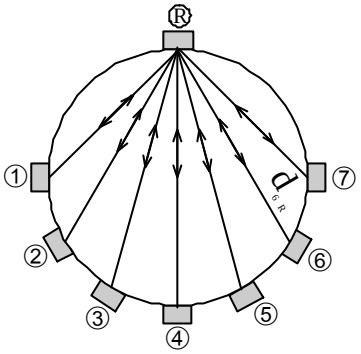

Figure 4. Transducers positions for a cross section of the pipe.

Two remarks can be done from this figure. The first one concerns the angle directivity of sources, especially ① and ⑦. In this configuration, the directivity is at least 90° while in ultrasonic flowmeters, this angle is much smaller, that is to say a better signal-to-noise ratio and so, better quality of the reception signal. The second is about the length of ultrasonic rays. In a flowmeter, it is generally $\sqrt{2}D$ and it could be easily increased by multiplying the number of reflections on the inner wall. Here, the minimal length is $D/\sqrt{2}$ and the maximal is D. Consequently, to obtain the same relative accuracy as for classical flowmeter in the determination of the time of flight measurement, the absolute accuracy has to be increased in the tomographic system.

In order to solve these problems, we have first chosen transducers which are able to emit a useful signal with an attenuation of less than 6 dB at an angle of 120°. Their frequency is 40 kHz and the diameter is 16 mm.

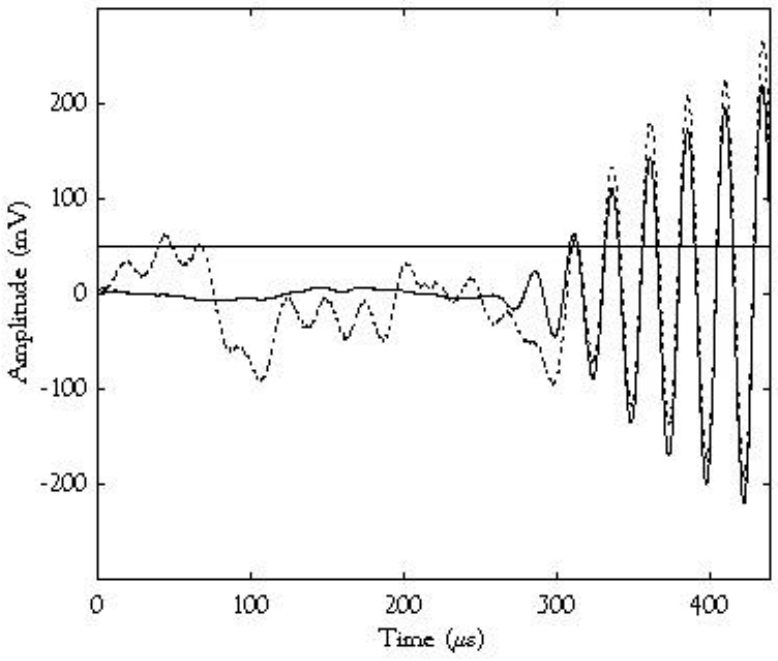

Figure 5. Comparison between raw signal and averaged signal.

Then, as suggested by Frøysa *et al.* [7], in order to reduce the noise which perturbs the reception signal, an average is operated on a certain number of signals. They are then recorded with an analogic-numeric converter and finally numerically averaged by a computer. Figure 5 shows the result of a 50 traces average for the couple ®-① of figure 4. The raw signal without treatment is represented with the dotted line (ð ð ð), and the averaged signal with the solid line (—).

In fact, in the meantime, this average can solve the problem of measurement accuracy of one transit time on a short distance. The method used for such averaged signals is said to be a “zero crossing ” method. It is the measurement of a first zero crossing point after the detection of a minimal

amplitude threshold. On figure 5, this threshold is materialised by the horizontal line situated at 50 mV. The exact time of propagation from source to receiver is obtained by the subtraction of the number of periods preceding this zero crossing (in the case of figure 5, two periods are omitted, i.e. 50 µs).
From this operating procedure, the developed method gets a satisfying accuracy that is to say, for 20 measures of transit time, the mean of the rms is about 2.5 ns whatever the separation length of transducers.

6 MEASUREMENT TOOL AND EXPERIMENTAL SETUP

6.1 Measurement tool

The measurement tool consists in two main parts. The first one (plane *a* on figure 2) allows to reconstruct the secondary flow (*Vx* and *Vy*) through the times of flight $T_1(a_i,a_j)$ defined in relation (8). The other one (plane *b*) joined to the first reconstitutes the axial flow (*Vz*) through $T_0(a_i,b_j)$ defined in relation (7).

The first part is one cross section perpendicular to the pipe axis. Its internal diameter is D=100mm and its length is 3D. Although there are only 8 transducers (see figure 4), the device can rotate around the conduit axis so, rather than limiting the distribution to one transducer at every 30°, experiences have been conducted considering one transducer every 10° (which is equivalent to a pipe with 36 transducers) [5].

Based on the same principle of rotation, the second part, 4D length, consists in two sections 1D apart (see figure 2). The distribution of transducers around each one is identical with the first part (see figure 4). Once again the transit times are measured between sensors of the two different sections. After a study on the incline of the transducers, we decided to fix all of them with an angle of 45° to the pipe axis (like in figure 1) in order to increase the ratio signal/noise.

Electronic instrumentation includes : a signal generator, a scanner to select the source transducer, a preamplifier-filter and an ADC installed in a PC which manages the signal acquisition and the reconstruction of the velocity profile.

6.2 Experimental set-up

The ultrasonic tomography device has been tested on the aerodynamic test bench described in figure 6. First of all, we used swirling flows created by a swirl generator which intensity is defined by the adimensional number W:

$$W = \frac{Q_{tangential}}{Q_{total}} \tag{13}$$

For all the experimental tests, the measurement tool is placed at a distance of 5D downstream of the swirler. The volume flow rate is Q_{total} = 200 $m^3.h^{-1}$ (i.e. mean velocity V_m in the order of 7.1 $m.s^{-1}$ in the section of measurement).

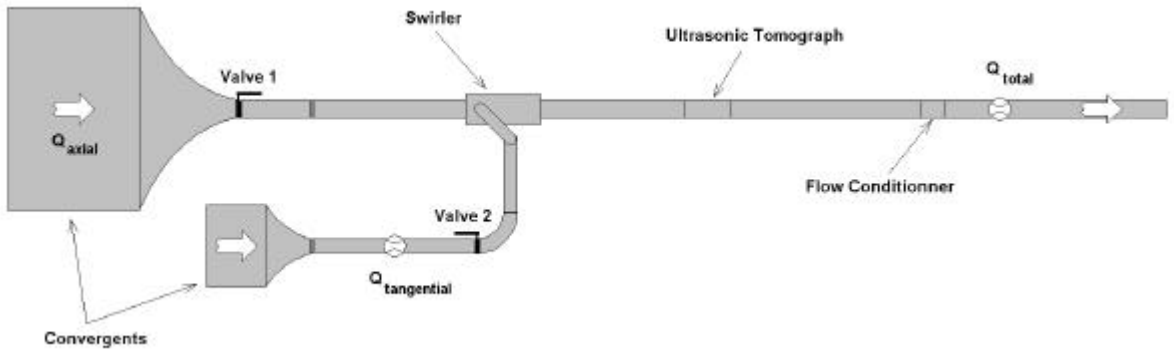

Figure 6. Testing bench.

7 EXPERIMENTAL RESULTS

For every configuration, the velocity profiles obtained from the tomographic reconstruction are represented in dotted line (- - -). These profiles are compared with the ones measured by a hot wire probe, in solid line (—). The velocity is normalised by the mean one V_m and the coordinates by the radius of the pipe R.

7.1 Fully developed flow

Closing the valve 1, only the axial flow exists and a fully developed flow is generated (see figure 6). The figure 7 represents the 3D view of the axial profile on the entire section of the pipe. In order to compare with hot wire measurements in the same conditions, the profile on a diameter is traced on figure 8. Near the wall, due to the lack of meshes in this region, important discrepancies appear. Then, the velocity is overvalued in the region near x/R = ±0.4. In fact, this problem depends typically on the method chosen to segment the ultrasonic paths on a cartesian mesh. However the reconstruction is better in the central part of the pipe.

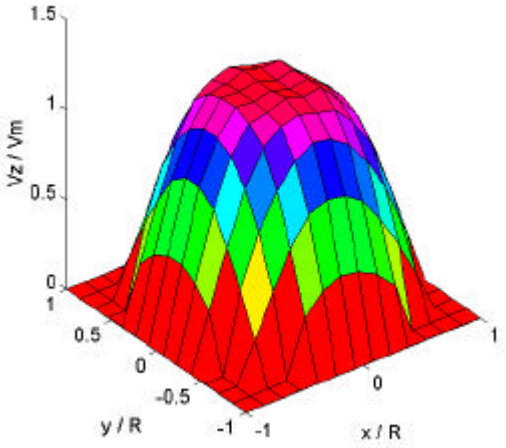

Figure 7. 3D axial velocity profile

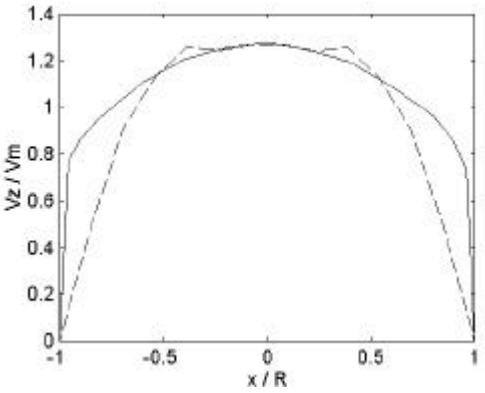

Figure 8. Axial velocity profile on a diameter

7.2 Swirling flows

We can adjust the opening of the valves 1 and 2 in order to control the introduction of the tangential flow rate in the main flow in order to obtain the intensity of swirl desired. The two configurations chosen are a weak rotation (W=0.2) and a strong rotation (W=0.8).

For W=0.2, the axial velocity profile is close to a fully developed profile. We can notice as in the previous case (part 7.1) the same difficulty to reconstruct the profile near the wall.

The tangential velocity (figure 10) can be decomposed in three parts : near the wall, strong gradients of velocity explain the difficulty in the reconstruction ; in the second part of the profile, near the two extrema, the two distributions are quite similar for x/R < 0 while the difference between the two profiles can reach about 12% for x/R > 0 ; a shift is present at the centre too. As regards the ultrasonic tomography, the profile is well centred on the pipe axis contrary to hot wire measurements.

For W=0.8, the axial profile is growing hollow on the pipe axis due to the centrifugal forces (figure 11). The tomography detects this decreasing of velocity, but the strong velocity gradients in this region are not well reconstructed.

The profile representing the secondary flow (figure 12) shows a good agreement between the two techniques despite the great velocity gradients on the two velocity components.

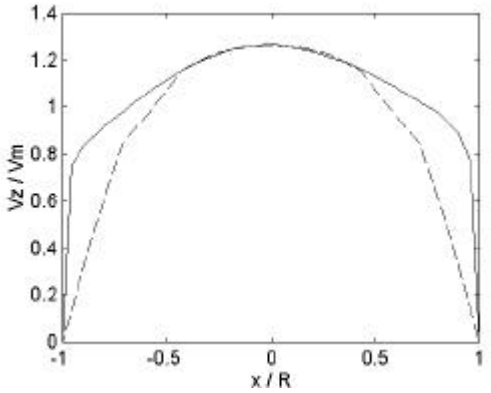

Figure 9. Axial velocity profile (W=0.2)

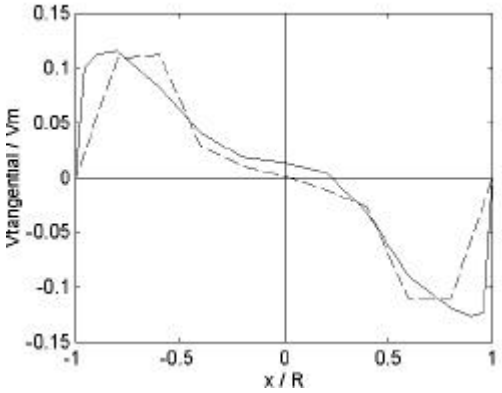

Figure 10. Tangential velocity profile (W=0.2)

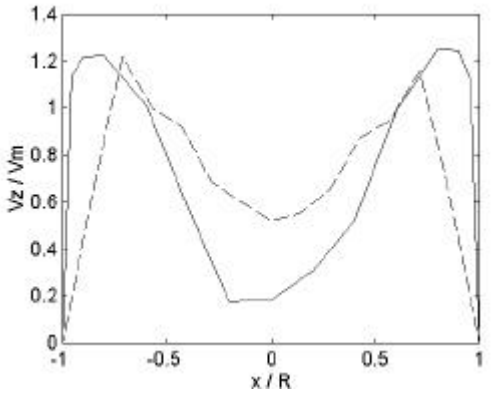

Figure 11. Axial velocity profile (W=0.8)

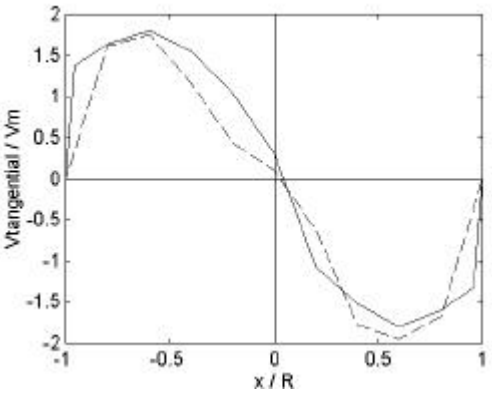

Figure 12. Tangential velocity profile (W=0.8)

7.3 Asymmetric flow

Asymmetry of the axial velocity profile is generated by an asymmetrical tube bundle, fixed on the bench just downstream of the swirler [10]. This disturbance is characterised by the asymmetry rate :

$$T_d = \frac{(Q)_{r<0} - (Q)_{r>0}}{(Q)_{ovl}} \times 100 \qquad (14)$$

where $(Q)_{r<0}$ and $(Q)_{r>0}$ are the flows calculated respectively over the negative and positive radius, and $(Q)_{ovl}$ is the flow calculated over the entire diameter. Here the maximum of T_d corresponds to the vertical diameter (figure 13). The profile obtained by hot wire measurements (—) gives a value of 19%. On the contrary, the velocity profile is quasi symmetrical ($T_d \approx 0$) over the horizontal diameter (figure 14).

Although there are differences between the profiles, the values of T_d are quite similar, respectively 20% and 1% with the ultrasonic tomography (ð ð ð).

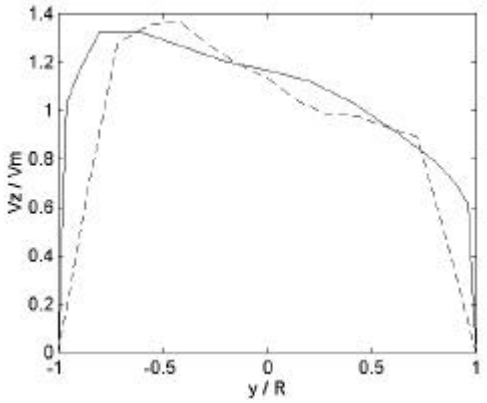

Figure 13. Axial velocity profile - Asymmetric flow (vertical diameter)

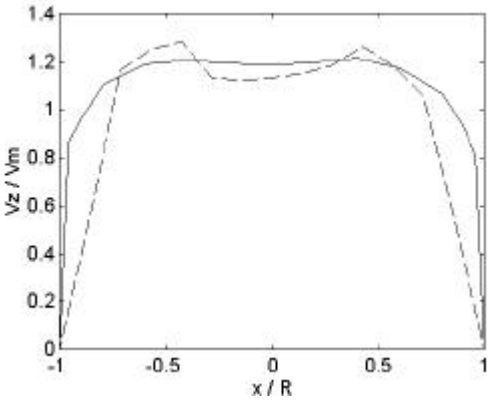

Figure 14. Axial velocity profile - Asymmetric flow (horizontal diameter)

8 CONCLUSION

A device using the ultrasonic tomography has been realised in order to reconstruct the secondary and the axial air flow profiles in a pipe. Measurements made in different flows (fully developed, swirling, asymmetric flows) have shown that this technique gives accurate results excepted in regions of flow where the velocity undergoes important velocity gradients. These results have been compared to hot wire measurements considered to be the velocity profiles reference.

The great difference between these two techniques is that hot wire anemometry can only measure the velocity profile along a diameter whereas the ultrasonic tomography device measures it over the whole section.

In order to illustrate this advantage and to show possibilities of such a device, others examples were conducted like the reconstruction of Dean vortices behind a 90° bend [5].

Even if the principle is near the one of USM, we had to improve the time of flight measurement for low level signal and specific transducers positions. Thus we developed a robust algorithm to reconstruct the flow profile.

As a conclusion, the ultrasonic tomography remains a good measurement technique in order to characterise the flow structures (swirl, asymmetry) that can be found in any industrial pipe flow metering device. Thus it could become a complementary tool to a flow meter to predict possible errors of metering.

But close to the pipe wall, we have a lower response from the present reconstruction software.

In the moment, we study the influence of a polar mesh in order to refine the mesh size in these regions. We are improving the response close to the wall and some tests are promising.

REFERENCES

[1] P. Lunde. K. E Frøysa, J. B. Fossdal, T. Heistad : " Functional enhancements within ultrasonic gas flow measurement ", *17th North Sea Flow Measurement Workshop*, Oslo, Norway, 25-28 October 1999.

[2] K. J. Zanker : " The effects of Reynolds number, wall roughness, and profile asymetry on single and multipath ultrasonic meters ", *17th North Sea Flow Measurement Workshop*, Oslo, Norway, 25-28 October 1999.

[3] T. A. Grimley : " The influence of velocity profile on ultrasonic flow meter performance ", *AGA 1998, Operation Conference*, Seattle, Washington, 1998.

[4] F. Vulovic, B. Harbrink, K. V. Bloemendal : " Installation effects on multi-path ultrasonic flow meters designed for profile disturbance ", *13th North Sea Flow Measurement Workshop*, Lillehammer, Norway, October 23-26, 1995.

[5] J. Démolis, J. Escande, P. Gajan, A. Strzelecki : " The use of ultrasonic tomography to characterize internal flows in pipes ", *9th International Conference on Flow Measurement*, *FLOMEKO'98*, Lund, Sweden, June 15-17, 1998.

[6] S. A. Johnson, J. F. Greenleaf, M. Tanaka, G. Flandro. : " Reconstructing three-dimensional temperature and fluid velocity vector fields from acoustic transmission measurements ", *ISA Transactions*, Vol. 16, No. 3, pp 3-15, 1977.

[7] K. E. Frøysa, P. Lunde, R. Sakariassen, J. Grendstad, R. Norheim : " Operation of multipath ultrasonic gas flow meters in noisy environments ", *14th North Sea Flow Measurement Workshop*, Scotland, 28-31 Octobre 1996.

[8] T. G. Herman : " Image reconstruction from projections, The fundamentals of computerized tomography ", *Academic Press, Inc. (London)*, 1980.

[9] J. Démolis : " Reconstruction du profil de vitesse d'un écoulement d'air en conduite par tomographie ultrasonore ", *Thèse de l'Ecole Nationale Supérieure de l'Aéronautique et de l'Espace*, 1997.

[10] A. Strzelecki. P. Gajan. D. Dutertre. V. de Laharpe. G. Mouton : " Performance of the new SMM flow conditioner ", *4rd International Symposium of Fluid Flow Measurement*, Denver, Colorado, U.S.A., June 28-30, 1999.

AUTHOR(S): PhD J. Escande, Eng Dr P. Gajan, Eng Dr A. Strzelecki, French Agency for Aerospace Research (ONERA) - BP 4025 - 31055 Toulouse Cedex 4 - France - tel. : +33(0)562 25 25 25.
E-mail: joel.escande@onecert.fr, pierre.gajan@onecert.fr, alain.strzelecki@onecert.fr.